The structure of the Ischia Volcanic Island from magnetic and gravity data

Valeria Paoletti[1,*], Maurizio Fedi[1], Giovanni Florio[1]

[1] *Department of Earth, Environment and Resources Science, University Federico II, Naples, Italy*

Article history
Received October 11, 2017; accepted November 27, 2017.
Subject classification:
Ischia Is.; Aeromagnetic data; Gravity data; Semblance analysis.

ABSTRACT

We carried out a study of the structures of the volcanic island of Ischia by the analysis and interpretation of high-resolution aeromagnetic data and by a newly compiled in-land gravity data set. The comparison between the vertical gradient of gravity data and pole-reduced magnetic data was performed through semblance analysis and highlighted a correspondence between the main magnetic and gravity highs over the lava and green tuff deposits (e.g., Punta Imperatore, Mt. Trippodi, Zaro, Mt. Rotaro, Mt. Epomeo). Our analysis also highlighted the simultaneous presence of a magnetic minimum and a gravimetric maximum in the central part of the island, mainly visible in the long-period components of the two data sets. This may be due to the existence of a partially demagnetized structure with positive density contrast, representing the island's igneous basement. The boundaries of the lava and tuffs deposits of the island were clearly pointed out by the maxima of the total horizontal gradient maps of magnetic and gravity data. Those maxima also show the position of several lineaments, in good agreement with the mapped faults of the island.

1. Introduction

The island of Ischia (Figure 1a) is the westernmost volcanic field of Phlegrean Fields, a volcanic area of Southern Italy that includes also Campi Flegrei and the island of Procida [Orsi et al. 1996]. These volcanoes, along with the Mt. Somma-Vesuvius complex, are known as the Neapolitan Volcanic Area. Except for Procida, all Neapolitan volcanoes, including Ischia, are still active, as testified by their historical eruptions and moderate seismicity, as well as hydrothermal and fumarole activity.

Ischia Is. (Figure 1b) is morphologically dominated by Mt. Epomeo (787 m a.s.l.) that is the morphological result of a prominent resurgence phenomenon taking place since ca. 33 ka BP [Orsi et al. 1991]. The resurgent block is ~ 4 x 5 km wide, and its edges are marked by a system of sub-vertical faults with NW-SE, NE-SW, and N-S strikes [e.g., Orsi et al. 1991, Tibaldi and Vezzoli 1998, Carlino 2012]. Several other faulty systems cut the deposits in the other sectors of the island [de Vita et al. 2006, Nappi et al. 2010] (Figure 1b). This structural setting seems to result from the interplay between regional and local tectonics [Orsi et al. 1991 and Acocella and Funiciello 1999].

The island is composed of volcanic rocks (mostly trachytes and phonolites, and minor shoshonites and latites; Figure 2a), marine sediments and landslide deposits [e.g., Vezzoli 1988, Orsi et al. 1992, D'Antonio et al. 2012]. The presence of these deposits is related to the interplay of tectonism, volcanism, erosion, sedimentation and slope instability throughout the island history [de Vita et al. 2006].

The oldest known products (>150 ka BP) are pyroclastic deposits cropping out at the south-eastern corner of Ischia, whereas lava domes and pyroclastic deposits of the activity between 150 and 75 ka crop out all around the periphery of the island [e.g., Vezzoli 1988 and references therein; Figure 2a). The main volcano-tectonic feature of Ischia is a caldera that formed about 55 ka BP during the Mt. Epomeo Green Tuff (MEGT) eruption [Orsi et al. 1991, Tibaldi and Vezzoli 1998]. The MEGT eruption emplaced an ignimbrite that covers much of the older deposits of the island [e.g. Vezzoli 1988] and emplaced also marine terrigenous formations in the central part of Ischia [Barra et al. 1992]. The last period began at about 10 ka with volcanism mostly within the eastern portion of the island [Orsi et al. 1991].

At about 6 ka BP, volcanism occurred also in the northwestern corner of the island (Zaro lava flows), outside the resurgent area, as a consequence of reactivation of regional faults. After a period of quiescence, volcanism resumed in the eastern portion of Ischia at

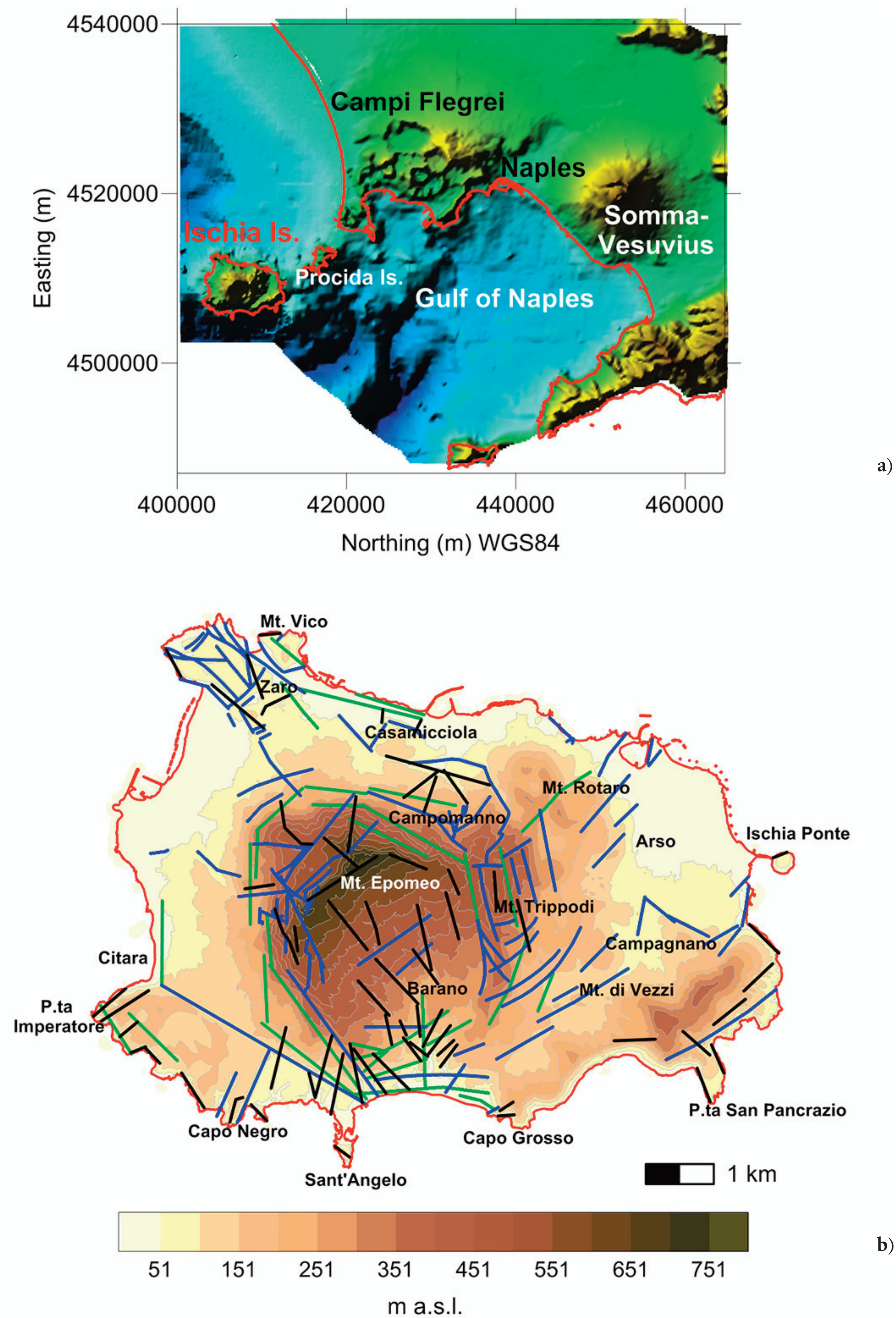

Figure 1. a) Neapolitan Volcanic Area; b) Topography of the Ischia Is. [from Nappi et al. 2010] with overlain structural lineaments from: Nappi et al. [2010] (black lines), De Vita et al. [2006] (blue lines), Acocella and Funiciello [1999] (green lines).

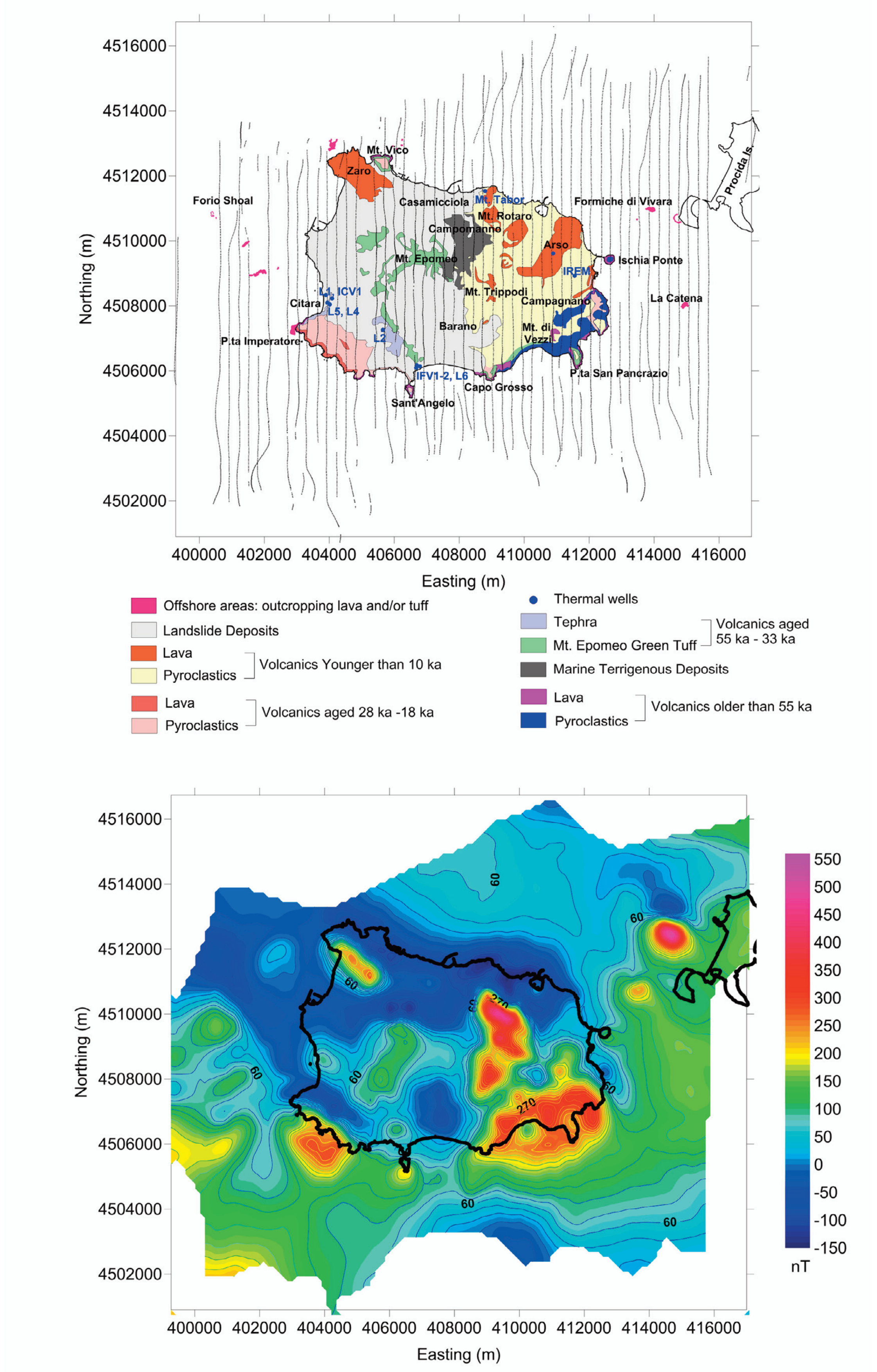

a)

b)

Figure 2. a) Helicopter-borne acquisition lines from the October 2005 high-resolution survey overlain to the geologic sketch map of Ischia. The geo-volcanological features of the island are from Vezzoli [1988], de Vita et al. [2006] and Paoletti et al. [2013]. The lava and/or tuff deposits of the offshore areas are from Budillon et al. [2003]. Blue dots show the thermal wells [Ippolito and Rapolla 1982 and references therein]. b) Aeromagnetic data of Ischia and its offshore surroundings.

about 5.5 ka BP and then again at 2.9 ka BP, with mostly trachytic magmas. The last eruption of the island occurred in 1302 AD (the Arso eruption in the island's eastern sector); [Buchner 1986].

The amount of information derived from geophysical data - and more specifically magnetic and gravimetric data - related to Ischia Island and its offshore surroundings is relatively poor. Until the eighties, the only magnetic data available for the Ischia area referred to an airborne survey carried out at regional scale (flight altitude of 2500 m and line spacing of 2000 m) [AGIP 1981] and to low resolution in-land magnetic and gravity surveys [Nunziata and Rapolla 1987, Paoletti et al. 2005].

Considering the lack of detailed geophysical data sets in the area, a high-resolution aeromagnetic survey was carried out over the island and its offshore surroundings in October 2005 (Figure 2) [Paoletti et al. 2009]. Furthermore, a new in-land gravimetric data set was compiled (Figure 3) [Fedi et al. 2011]. In this paper, we present a study of the geo-structural setting of the island of Ischia based on the combined analysis of these datasets. We support our interpretation by a previous modeling of potential field data and by the temperature data measured in deep thermal wells of the island [Paoletti et al. 2015].

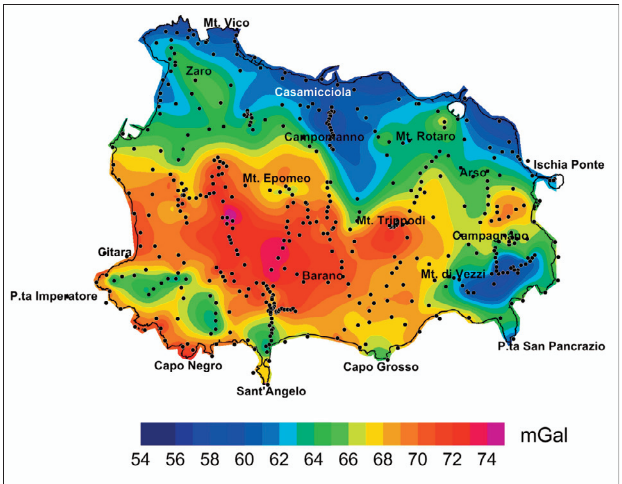

Figure 3. Bouguer gravity anomalies of Ischia, including the newly collected in-land gravity stations [Fedi et al. 2011]. Black dots mark the position of the gravity stations.

2. The Magnetic Field of the Ischia Island

2.1. Aeromagnetic Data Layout and Processing

The high-resolution helicopter-borne magnetic survey, carried out in October 2005, covered the entire area of the island of Ischia, extending also in the offshore zones (Figure 2a). The flight lines, with a N-S azimuth, were spaced 300 m apart, whereas the cross-track tie lines, with a E-W azimuth, were spaced about 4000 m apart. The sample spacing along each flight line was about 5 m. The survey was flown at a constant terrain clearance of about 300 m. To avoid numerical problems during the successive gridding, which could be connected to the different detail of data along the N-S and E-W directions, we re-sampled the data along each line with a spacing of 50 m.

The instrumentation used for the survey was supplied by the *Geological Survey of Austria* and consisted of a ground and a flight section. The ground section contained a magnetometer used to monitor the external field activity during the flights and a GPS reference station used for the differential correction of satellite data. The flight section consisted of:

i) a caesium magnetometer having a sensitivity of 0.01 nT, which was contained in a "bird" dragged 30 m below the helicopter;
ii) a GPS sensor for the horizontal positioning of the helicopter, having a precision of ± 5 m after correction by satellite data;
iii) a laser-altimeter for the vertical positioning of the helicopter;
iv) a computer for data acquisition;
v) a video-camera.

The processing of the aeromagnetic data set measured over the island of Ischia included:

i) removal of spikes and gaps in the data;
ii) flight path check and repositioning, which consisted in the removal of wrong coordinates, correction of the GPS data, and check of the flight altitude;
iii) Earth's magnetic field diurnal variation correction, which was performed using the local base station data;
iv) removal of the *International Geomagnetic Reference Field* (IGRF);
v) statistical leveling, consisting in a minimization of the differences between the field values measured at the crossing points of flight lines and tie lines.

2.2. Data Presentation and Analysis

After the data correction procedure, the aeromagnetic data were gridded to an interval of 150 m by using the Kriging algorithm. The map obtained (Figure 2b) is characterized by prominent anomalies with amplitude of 400-600 nT, both onshore and offshore. Some of the anomalies onshore seem to correlate with the main geo-volcanological characteristics of the island, such as domes and lava flows, and of the offshore areas (see geological map of Figure 2a). Other anomalies, onshore and offshore, seem instead uncorrelated to both

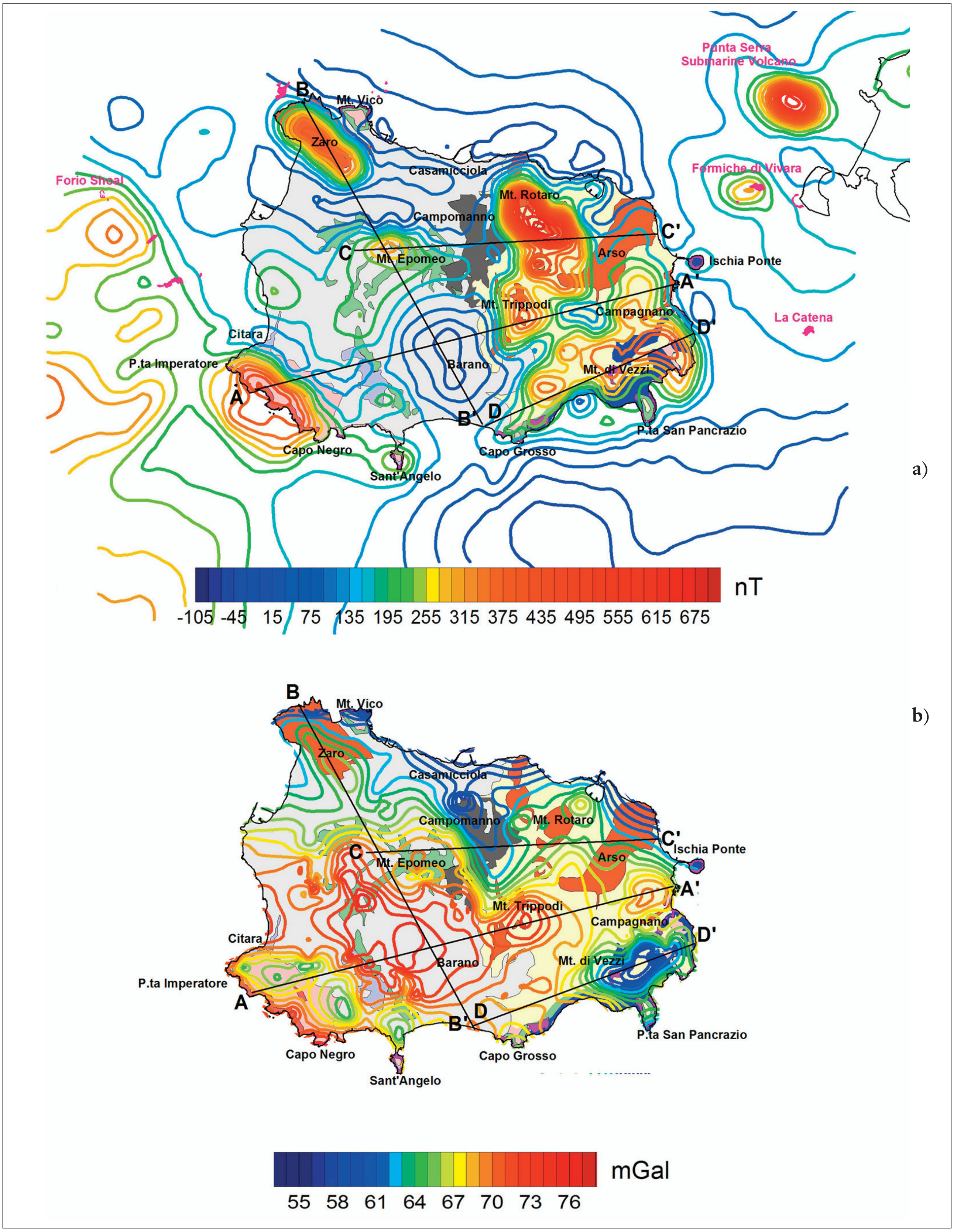

Figure 4. Pole-reduced magnetic data (a) and gravimetric data (b) overlain on a volcanological sketch map of the island (refer to Figure 2a for details). The lines show the location of profiles analyzed in Figs. 5-8.

geological and topographical/bathymetric features. A comparison between the new data and the two previous, airborne and in-land, data sets (Figure 1) shows how the new aeromagnetic data allow a much more detailed definition of the characteristic - amplitude and shape - of the anomalies of the island and its offshore areas.

In order to locate the position of the magnetic sources of the observed anomalies, we computed a pole-reduced map (Figure 4a), using the direction of the present inducing field in the area (inclination = 56°; declination = 2°) for the induced and total magnetization vectors. We did not account for remanent magnetization as the oldest known products are more recent than the last inversion of the Earth's Inducing Magnetic Field. The so-obtained anomalies correlate well with the main volcanological features of the island. The most prominent maxima of the field are placed in correspondence with the lava deposits younger than 10 ka, such as Zaro, Mt. Rotaro, Mt. Trippodi, and the older (28 ka - 18 ka) lava deposits on the coast between Pt. Imperatore and Capo Negro. These anomalies show an amplitude of about 400 nT, 750 nT, 300 nT and 450 nT, respectively. The 1302 AD Arso eruption products (lava flows and tephra), on the other hand, seems not to be associated with any relevant anomaly. This could be possibly related to the relatively small volume and textural character of these deposits, composed of both lava flows and tephra (0.03 km^3) [de Vita et al. 2010 and references therein]. Smaller anomalies, showing amplitudes of about 60 nT, 100 nT and 280 nT are located over the lavas older than 55 ka of Ischia Ponte, Sant'Angelo and Mt. di Vezzi, respectively. The Mt. Epomeo is characterized by an anomaly of about 340 nT, related to the tuffs of the area.

In the offshore areas, we note only a few relevant anomalies: one is located in correspondence with the shoal of Forio, exhibiting an amplitude of 280 nT; other two maxima are placed in the offshore area west of Procida. These anomalies are very likely connected to the *Formiche di Vivara volcano* (amplitude of 160 nT) and to the *Ruommoli Volcano* [Putignano and Schiattarella 2010]. A magnetic modeling of these two anomalies showed that they are connected to two dyke-like igneous bodies extending to a depth of several hundred meters b.s.l. [Paoletti et al. 2008]. The analysis of marine magnetic and seismic data [Bruno et al. 2002] showed that probably old volcanic structures related to the Ischia magmatism extend westward as submarine bathymetric reliefs in an area as large as that of the island itself.

The newly compiled Bouguer anomaly map of the island (Figure 3) [Fedi et al. 2011] was obtained by integrating older data from the 1960s [Maino and Tribalto 1971] with data acquired in 1999 by a LaCoste & Romberg mod. D-137 gravimeter, and using a density value for the island's deposits of 1.8 g/cm^3.

The map was obtained gridding the data by the kriging interpolation method, with a grid-node spacing of 150 m. It shows a regional trend with decreasing values from South to North, on which a series of anomalies related to local sources is superimposed. Remarkable features are:

i) A main positive anomaly over the center of the island, extending from Mt. Epomeo to Barano;
ii) Several isolated positive anomalies in the areas of Zaro, Citara, Mt. Rotaro, Trippodi, Arso;
iii) A main negative NNW-SSE trending anomaly at Casamicciola-Campomanno;
iv) Some isolated negative anomalies around Pt. Imperatore, Capo Negro and S. Angelo, and in the area of Monte di Vezzi.

To analyze possible, positive or negative, correlations between magnetic and gravity anomalies over Ischia, we first performed an upward continuation of the two datasets from their respective draped acquisition surfaces to a common flat surface [Ridsdill-Smith, 2000].

Then we compared the pole-reduced magnetic data with the vertical gradient of gravity data along four profiles crossing the main anomalies of the island (Figure 4).

The geologic basis for such a correlation analysis is the expectation that lateral variations in composition and physical properties of crustal rocks are reflected in both the bulk mineralogy and in the content of magnetite or other accessory magnetic minerals [von Frese et al. 1997b]. The bulk mineralogy controls the rock density and hence its lateral variation determines the occurrence of gravity anomalies, while the volume percentage of magnetite determines the occurrence and the amplitude of magnetic anomalies. The correlation between gravity and magnetic anomalies is often computed in the Fourier domain by computing the cosine of the difference between the Fourier phase angles of the two datasets, at each wavenumber *k* [von Frese et al. 1997a]:

$$SF(k) = \cos(\Delta\theta_k) = \frac{\bar{A}(k)\cdot\bar{B}(k)}{|\bar{A}(k)||\bar{B}(k)|} \qquad (1)$$

where $\bar{A}(k)$ e $\bar{B}(k)$ are the Fourier transforms of the signals a(x) and b(x), $|\bar{A}(k)|$ and $|\bar{B}(k)|$ are their amplitudes and $\Delta\theta_k$ is the phase difference vector of the two transforms at each wavenumber.

We performed instead a signals' phase comparison as a function of both space and wavelength through a wavelet transform-based semblance analysis as defined by Cooper and Cowan [2008], exploiting the space-scale properties of the continuous wavelet transform (CWT). In the wavelet framework, the semblance *S* is defined as:

$$S = \cos\theta \qquad (2)$$

where $\theta = \tan^{-1}\left(\frac{I(CWT_{1,2})}{R(CWT_{1,2})}\right)$, *I* and *R* denote, respectively, the imaginary and real part of the Continuous Wavelet Transform (CWT) and $CWT_{1,2} = CWT_1 \cdot CWT_2^*$, where the symbol * stands for the complex conjugate, and CWT_1 and CWT_2 are, respectively, the CWT of the first and second dataset. The semblance can have values between -1 and 1, corresponding, respectively, to a perfect phase anticorrelation and a perfect phase correlation between the two data-series. A value of 0 implies the absence of any positive or negative correlation.

Our semblance analysis of magnetic *vs*. gravity data along the four profiles (Figure 4) showed:

- Profile A-A' (Figure 5): a marked anticorrelation at the longest wavelengths and at shorter wavelengths (2000-4000 m) in the western part; a general positive correlation at intermediate wavelengths, mainly in the eastern part of the profile;
- Profile B-B' (Figure 6): an anticorrelation between the gravity and magnetic data at the longest wavelengths in the south-eastern part of the profile and a positive correlation in its north-western part and at shorter wavelengths;
- Profile C-C' (Figure 7): a clear positive correlation between the gravity and magnetic data at the longest wavelengths and an anticorrelation at shorter wavelengths in the western part of the profile;
- Profile D-D' (Figure 8): a diffuse anticorrelation of the gravity and magnetic data at each wavelength with some high correlation in the western part of the profile for the longest wavelengths and in some central portions of the profile at shorter wavelengths.

The simultaneous presence of magnetic minimum and gravimetric maximum in the central part of the island (shown in profiles A-A' and B-B') may be explained as related to the existence of a demagnetized basement with positive density contrast (see Section 2.3). As regards the short wavelengths signals, we note

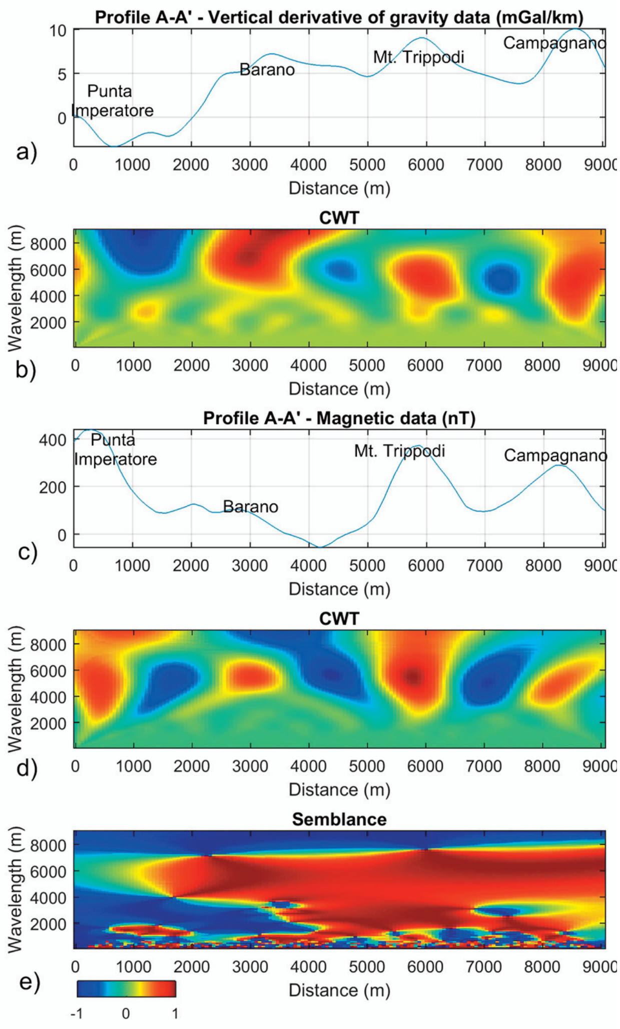

Figure 5. Semblance analysis along profile A-A' (see text for details). a) Gravity data; b) CWT of the gravity data; c) magnetic data; d) CWT of magnetic data; e) semblance function obtained by the processing of the two CWT according to Equation 2.

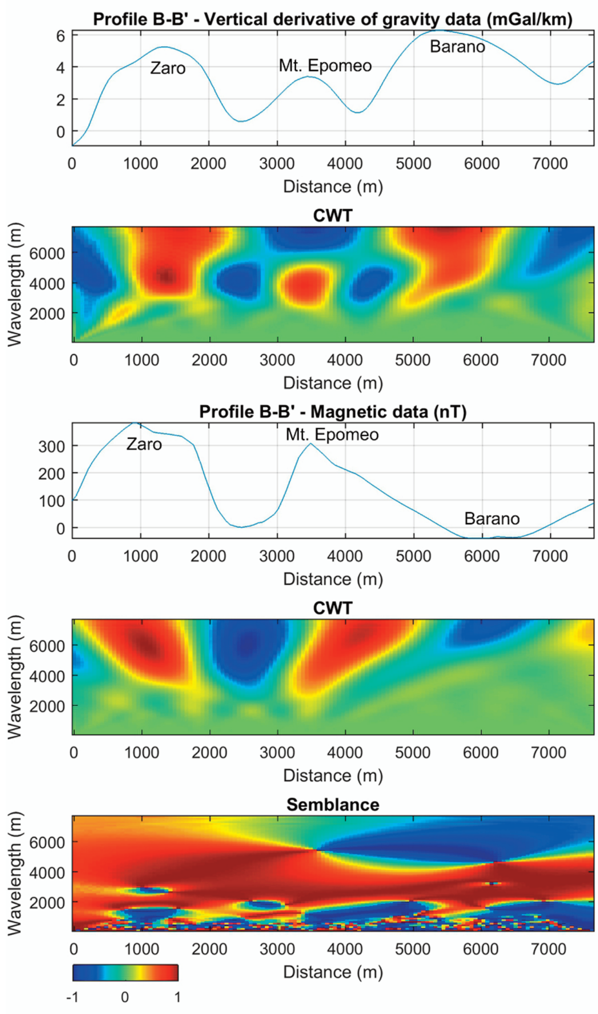

Figure 6. The semblance analysis along profile B-B'. a) Gravity data; b) CWT of the gravity data; c) magnetic data; d) CWT of magnetic data; e) semblance function obtained by the processing of the two CWT according to Equation 2.

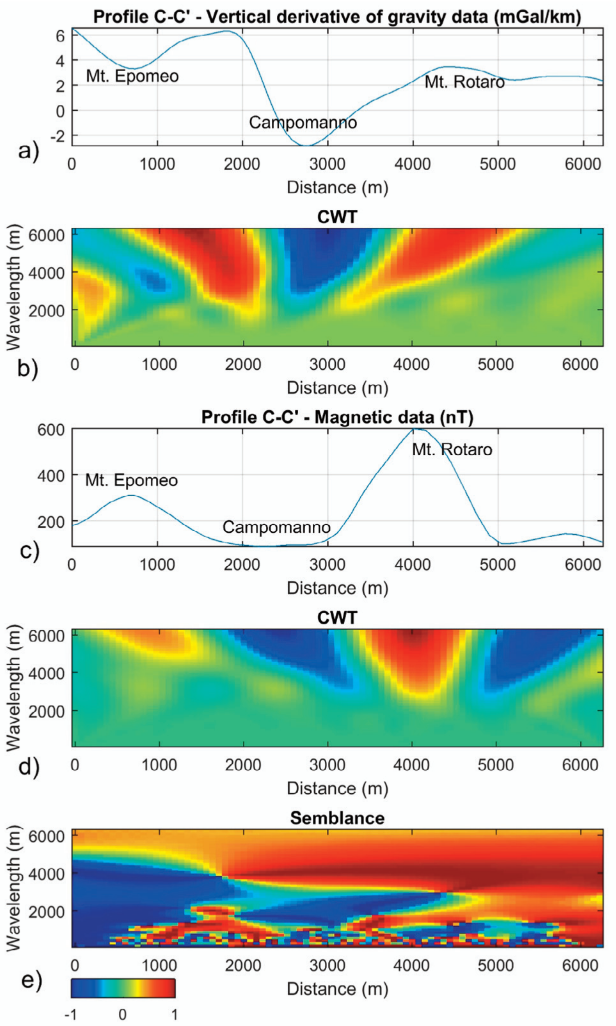

Figure 7. The semblance analysis along profile C-C'. a) Gravity data; b) CWT of the gravity data; c) magnetic data; d) CWT of magnetic data; e) semblance function obtained by the processing of the two CWT according to Equation 2.

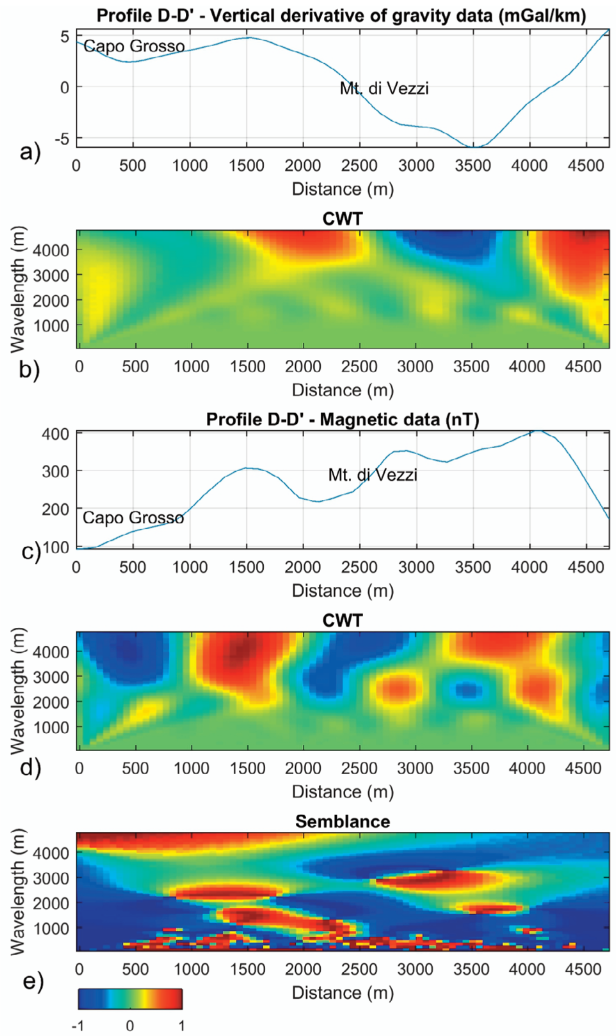

Figure 8. The semblance analysis along profile D-D'. a) Gravity data; b) CWT of the gravity data; c) magnetic data; d) CWT of magnetic data; e) semblance function obtained by the processing of the two CWT according to Equation 2.

that the pole-reduced magnetic and gravity highs in the areas of Zaro, Punta Imperatore, Mt. Trippodi and Mt. Rotaro (profiles A-A', B-B', C-C' and D-D', Figures 5-8) are due to the presence of lava deposits, whereas the positive anomalies in Mt. Epomeo are related to green tuff deposits. The magnetic and gravity lows in Campomanno seem related to the presence of terrigenous deposits (profile C-C', Figure 7), whereas the simultaneous presence of a magnetic high and gravity low in the Mt. di Vezzi area (profile D-D', Figure 8) may be attributed to the existence of a collapse structure placed just under the mount [Paoletti et al. 2007]. The boundaries of the above described sources are clearly highlighted by the total horizontal gradient maxima of the pole-reduced magnetic field (M-THG, Figure 9a) and by the total horizontal gradient maxima of gravity data (G-THG, Figure 9b). The M-THG and G-THG maxima also show the position of faults contacting lithologies with different magnetization and/or densities.

2.3. Deep Structure

In order to provide insights into the deeper and larger magnetic structures of Ischia, we analyzed the long-period field components by performing an upward continuation of the pole-reduced magnetic data and of gravity data from a draped surface to a constant altitude of 1500 m a.s.l. [Ridsdill-Smith 2000]. Figure 10 shows a comparison between the total gradient of the upward continued magnetic data, pointing out the horizontal position of the island's larger and deeper sources [e.g. Roest et al. 1992], and the upward continued gravity data.

The total gradient of the upward continued magnetic field (Figure 10a) highlights the existence of large-scale magnetic sources in the eastern area of the island and a smaller one in the south-western coast, whereas there is no evidence of magnetic sources in the central sector of the island. The long-period gravity data show instead a maximum in the central-western sector of Ischia (Figure 10b). The lack of a clear magnetic signa-

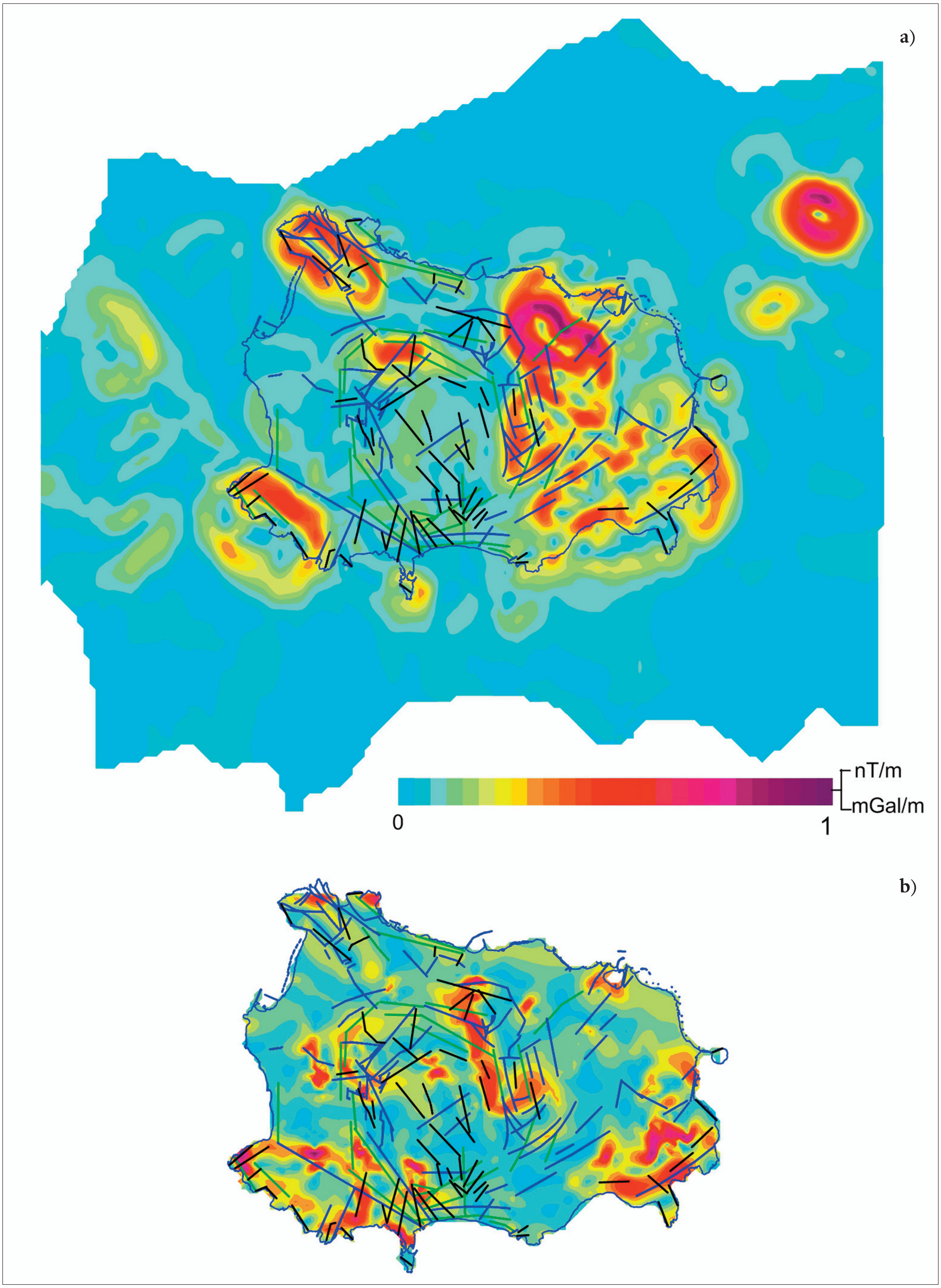

Figure 9. Maps of the horizontal gradient of the magnetic and gravity data at Ischia, highlighting the location of magnetic/density lineaments: a) Total horizontal gradient of the pole-reduced aeromagnetic data (M-THG); b) Total horizontal gradient of gravity data (G-THG). The values of the two THG datasets are normalized. Structural lineaments are from: Nappi et al. [2010] (black lines), De Vita et al. [2006] (blue lines), Acocella and Funiciello [1999] (green lines).

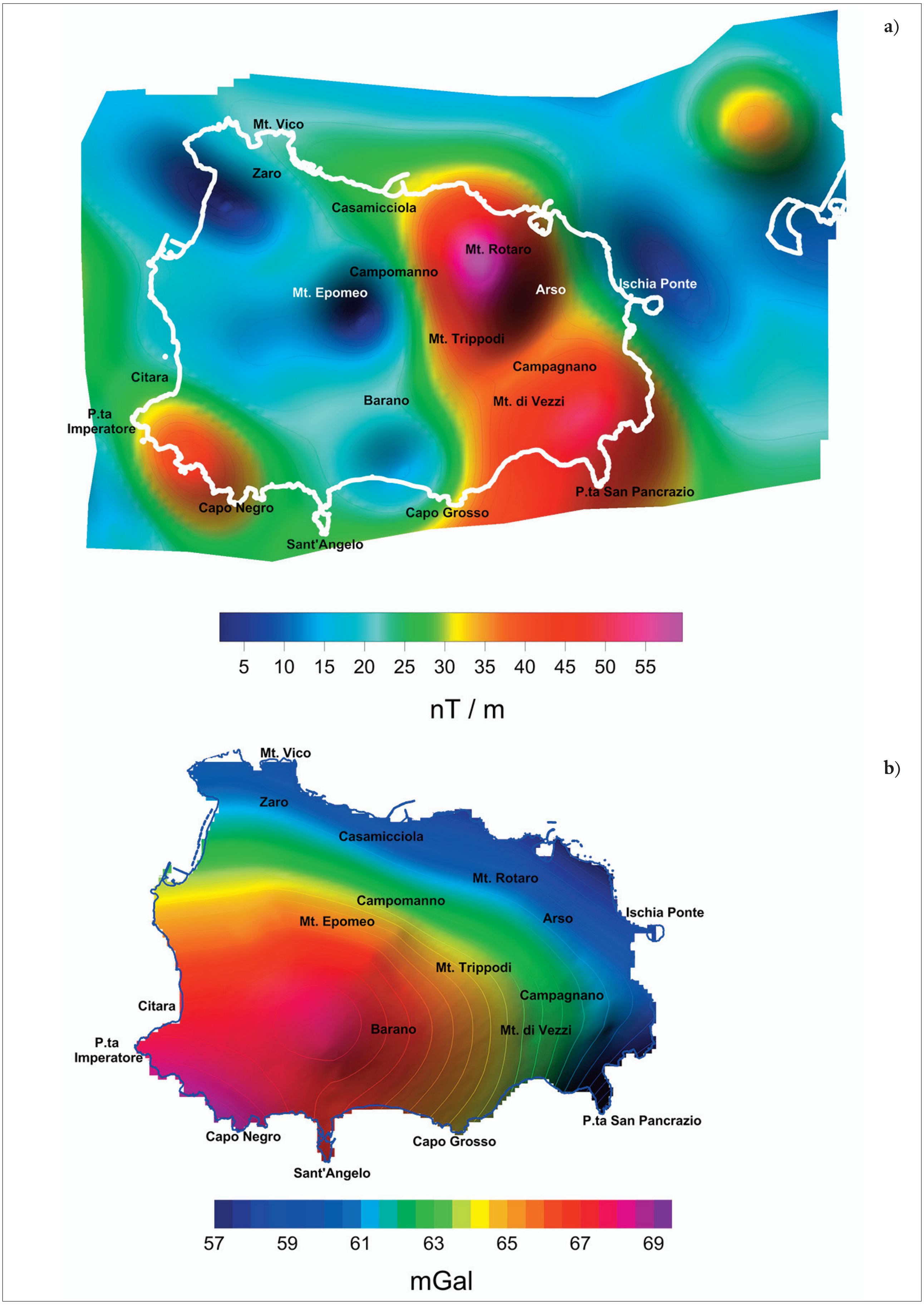

Figure 10. Maps of the two datasets after upward continuation at 1500 m a.s.l., highlighting the horizontal position of large scale sources: a) Total gradient of the pole-reduced aeromagnetic data; b) Gravimetric data.

ture in the central sector of Ischia and the simultaneous presence of a gravimetric maximum there (visible also in the shorter scale components, see Figs. 5-6, profiles AA' and BB') may ascribed to the high geothermal gradient of the south-western sector of the island, as measured in deep wells [e.g. Ippolito and Rapolla 1982].

This result was confirmed by a recent study on the geothermal potential of the island [Paoletti et al. 2015], which highlighted the south-western sector of the island as the most suitable zone for power plants installations. A joint modeling of the magnetic and gravity long-period components along a profile [Paoletti et al. 2013] pointed out the presence of a structure with a density of 2.4 g/cm3 and variable magnetization, whose top is located at 1200-1750 m b.s.l.

While in the eastern and western areas of the structure the magnetic data modeling showed the presence of magnetized material, the central-western part of the basement structure, under Mt. Epomeo-Barano, seems demagnetized.

This could be due to hydrothermal alteration phenomena of the igneous materials, related to the high geothermal gradient measured in the wells located in the south-western sector of the island and/or the presence of partially molten areas inside the basement. This structure is probably trachytic, as suggested by findings in drillings carried out in the south-western side of the island [Penta and Conforto 1951] and could be interpreted as the basement of the island.

3. Conclusions

We carried out a study of the structures of the Island of Ischia by the coupled analysis of high-resolution aeromagnetic data and a recently compiled in-land gravity data set. The detail of our study was influenced by the spacing of data acquisition and data interpolation of the two datasets. Given the surveys layouts, a grid-node spacing of 150 m was appropriate for interpolating data of both datasets. The computation of the pole-reduced map of the magnetic data showed that the maxima of the field are mainly located in correspondence with the island's lava deposits younger than 10 ka and highlighted some interesting off-shore anomaly sources. A semblance analysis of magnetic and gravity data along four profiles crossing the most prominent anomalies of the island pointed out a correspondence between magnetic and gravity highs over the lava and green tuff deposits (e.g., in the areas of Punta Imperatore, Mt. Trippodi, Zaro, Mt. Rotaro, Mt. Epomeo).

The boundaries of these deposits, and the position of faults contacting lithologies with different magnetization and/or densities, were clearly pointed out by the maxima of the total horizontal gradient of both data sets.

Our comparison analysis also showed a simultaneous presence of a magnetic minimum and a gravimetric maximum in the central part of the island. This correspondence was studied through the analysis of the

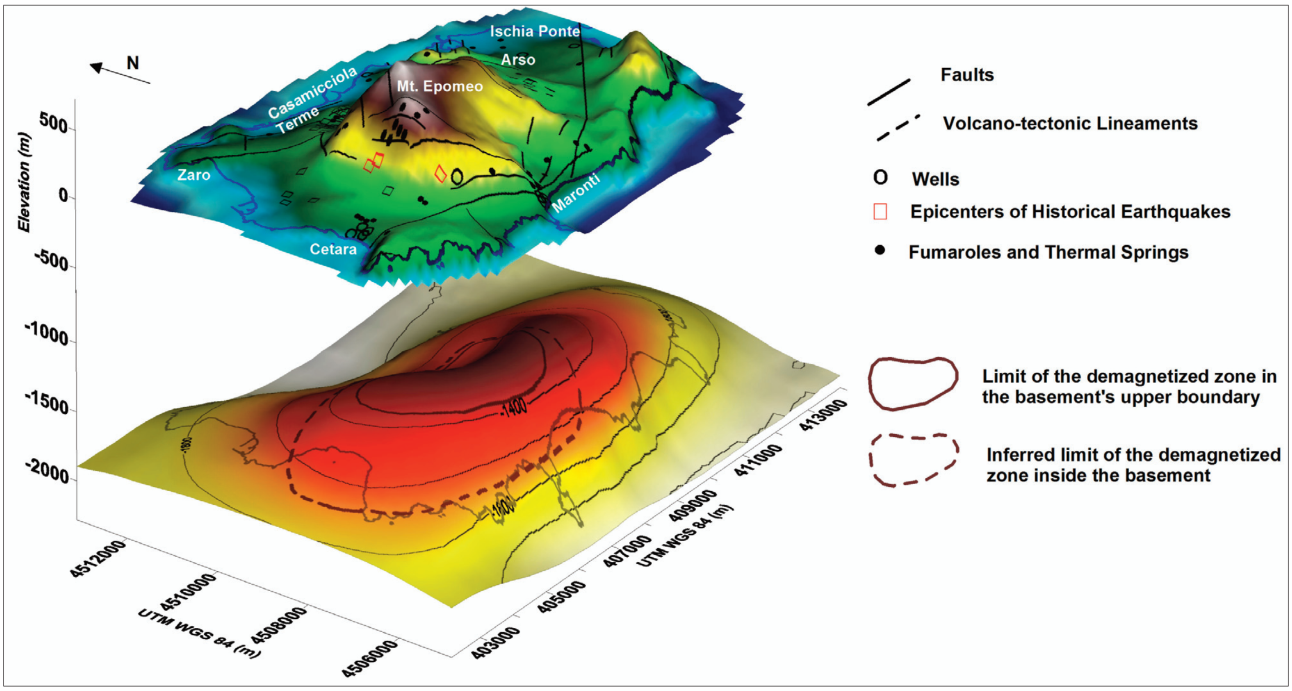

Figure 11. Pattern of the Ischia's basement inferred from gravimetric modeling [Nunziata and Rapolla 1987]. Demagnetized areas were identified based on magnetic modeling [Paoletti et al. 2009]. The main faults and volcano-tectonic lineaments area redrawn from Acocella and Funiciello [1999]. Fumaroles, thermal springs and historical earthquakes epicenters are from Manzo et al. [2006], Wells are from Ippolito and Rapolla [1982].

long-period (upward continued) field components and was explained as related to the existence of a partially demagnetized structure, with positive density contrast, representing the island's igneous basement. The basement's demagnetization could be possibly due to alteration processes of the igneous materials connected to the high temperatures measured in the wells of the central-western sector of the island. Regarding this hypothesis, Nunziata and Rapolla [1979] have shown that for a body of size x=1000 m, z=3500 m and y=∞, after about 30 ka, the temperatures at 1000 m from the surface of the body are about 150°C. This value agrees with the temperature measured in the deepest well of the island (over 200°C at 1150 m b.s.l.) considering the larger dimensions of the demagnetized body shown by the modeling.

Thus, we can infer that while most of the basement is cold enough to generate a magnetic field, significant portions of it may still experience high temperatures and/or be demagnetized. In Figure 11 we present a sketch of the island basement and show a possible pattern of the demagnetized volume inside the basement, here inferred based on the evidence that the highest temperatures were measured in wells located in the south-western sector of the island. This hot central sector of the island basement may represent the thrust for the Mt. Epomeo block's resurgence.

Acknowledgements. We are grateful to two anonymous reviewers whose constructive suggestions were a great help in improving our paper.

References

Acocella, V. and R. Funiciello (1999). The interaction between regional and local tectonics during resurgent doming: The case of the island of Ischia, Italy. J Volcanol Geotherm Res., 88, 109-123.

AGIP (1981). Carta aeromagnetica d'Italia scala 1:5000000: fogli G, H, L, M. Attività Mineraria, Direzione Esplorazione Idrocarburi, S. Donato Milanese, Italy (in Italian).

Barra, D., A. Cinque, A. Italiano and R. Scorziello (1992). Il Pleistocene superiore marino di Ischia: paleoecologia e rapporti con l'evoluzione tettonica recente. Studi Geol. Camerti, 1, 231-243 (in Italian).

Bruno, P.P.G., G. De Alteriis and G. Florio (2002). The western undersea section of the Ischia volcanic complex (Italy, Tyrrhenian Sea) inferred by marine geophysical data. Geophysical Research Letters, 29(9), 1-4.

Buchner, G. (1986). Eruzioni vulcaniche e fenomeni vulcano-tettonici di eta' preistorica e storica nell'isola d'Ischia. In: Eruptions Volcaniques, Tremblemants de Terre et Vie des Hommes dans la Campanie Antique. Centre J. Bérard, Inst. Fr. de Naples, Naples, Italy, vol. 7, pp. 145-188 (in Italian).

Budillon, F., C. Violante, M. De Lauro, L. Ferraro and F. Molisso (2003). Carta geologica dei fondali delle isole flegree. In: Ambiente marino costiero e territorio delle isole flegree (Ischia, Procida e Vivara) e Golfo di Napoli. Risultati di uno studio multidisciplinare. Monografia Accademia di scienze Matematiche, Fisiche e Naturali, Liguori Ed., Naples (in Italian).

Carlino, S., (2012). The process of resurgence for Ischia Island (southern Italy) since 55 ka: the laccolith model and implications for eruption forecasting. Bull. Volcanol., 74, 947-961.

Carlino, S., E. Cubellis, G. Luongo and F. Obrizzo (2006). On the mechanics of caldera resurgence of Ischia Island (southern Italy). In: Troise, C., G. De Natale and C.RJ. Kilburn (Eds.), Mechanisms of Activity and Unrest At Large Calderas. Geol. Soc. London Sp Publ., 269, 181-193.

Cooper, G.R.J. and D.R. Cowan (2008). Comparing Time Series using Wavelet Based Semblance Analysis. Computers & Geosciences, 34(2) 95-102.

de Vita, S., F. Sansivero, G. Orsi and E. Marotta (2006). Cyclical slope instability and volcanism related to volcano-tectonism in resurgent calderas: The Ischia island (Italy) case study. Eng. Geol., 86, 148-165.

Fedi M., G. Florio, M. Grimaldi and F. Italiano (2011). La nuova carta di Anomalie Di Bouguer dell'Isola d'Ischia, in: Sbrana, A. and R.M. Toccaceli (eds.), Carta Geologica dell'Isola d'Ischia con note illustrative, Scala 1:10000. Regione Campania (in Italian).

Ippolito, F. and A. Rapolla (1982). L'energia geotermica in Campania. In: Fonti Energetiche Alternative, Fondazione Politecnica per il Mezzogiorno. Franco Angeli Ed., Milano, 57-106 (in Italian).

Maino, A. and G. Tribalto (1971). Rilevamento gravimetrico di dettaglio dell'isola d'Ischia (Napoli). Boll. Serv. Geol. It., 92, 109-123 (in Italian).

Manzo, M., G.P. Ricciardi, F. Casu, G. Ventura, G. Zeni, S. Borgstrom, P. Berardino, C. Del Gaudio and R. Lanari (2006). Surface deformation analysis in the Ischia Island (Italy) based on spaceborne radar interferometry. J Volcanol. Geotherm. Res., 151, 399-416.

Nappi R., G. Alessio, E. Bellucci Sessa (2010). A case study comparing landscape metrics to geologic and seismic data from the Ischia Island (Southern Italy). Applied Geomatics, 2:73-82, DOI: 10.1007/s12518-010-0023-z.

Nunziata, C. and A. Rapolla (1979). Analysis and synthesis of the geological, geophysical and volcanological data about the Neapolitan area and its geothermal potential (part I). Rapporto EUR 6152 E/F, MF, Commissione delle Comunità Europee, Direzione Generale per la Ricerca, Scienza ed Educazione, 22 pp.

Nunziata, C. and A. Rapolla (1987). A gravity and magnetic study of the volcanic island of Ischia, Naples (Italy). J. Volcanol. Geotherm. Res., 3, 333-344.

Orsi, G., G. Gallo, A. Zanchi (1991). Simple-shearing block resurgence in caldera depressions. A model from Pantelleria and Ischia. J. Volcanol. Geotherm. Res., 47, 1-11.

Orsi, G., S. de Vita S. and M. di Vito (1996). The restless resurgent Campi Flegrei nested caldera (Italy): constraints on its evolution and configuration. J. Volcanol. Geotherm. Res., 74, 179-214.

Paoletti, V., M. Secomandi, G. Florio, M. Fedi and A. Rapolla (2005). The integration of remote sensing magnetic data in the Neapolitan volcanic district. Geosphere, 1, 85 96.

Paoletti, V., A. Rapolla and M. Secomandi (2007). The structural setting of the Monte di Vezzi area, Ischia Island, derived from geophysical data. Italian Journal of Engineering Geology and Environment, 2, 15-26.

Paoletti, V., A. Rapolla and M. Secomandi (2008). Magnetic signature of submarine volcanoes in the Phlegrean Fields-Ischia Ridge (North-Western side of the Bay of Naples, Southern Italy). Ann. Geophys., 51, 575-584.

Paoletti, V., R. Di Maio, F. Cella, G. Florio, K. Mocka, N. Roberti, M. Secomandi, R. Supper, M. Fedi and A. Rapolla (2009). The Ischia Volcanic Island (Southern Italy): Inferences from Potential Field Data Interpretation. J. Volcanol. Geotherm. Res., 179, 69-86.

Paoletti, V., M. D'Antonio and A. Rapolla (2013). The Structural Setting of the Ischia Island within the Neapolitan Volcanic Area: Inferences from Geophysics and Geochemistry. J. Volcanol. Geotherm. Res., 249, 155-173.

Paoletti, V., G. Langella, R. Di Napoli, A. Amoresano, S. Meo, G. Pecoraino, A. Aiuppa (2015). A tool for evaluating geothermal power exploitability and its application to Ischia, Southern Italy. Applied Energy, 139, 303-312.

Penta, F. (1954). Ricerche e studi sui fenomeni esalativi-idrotermali e il problema delle forze endogene. Ann. Geofis., 8, 1-94 (in Italian).

Penta, F. and B. Conforto (1951). Risultati di sondaggi e di ricerche geominerarie nell'isola d'Ischia dal 1939 al 1943, nel campo del vapore, delle acque termali e delle 'forze endogene' in generale. Ann. Geofis., 4, 159-191 (in Italian).

Putignano, M.L. and M. Schiattarella (2010). Geomorfologia strutturale e domini di frattura dei fondali marini pericostieri dell'Isola di Procida (Campi Flegrei insulari, Italia Meridionale). Il Quaternario 23(2Bis), Volume Speciale, 229-242.

Rapolla, A., M. Fedi and M.G. Fiume (1989). Crustal structure of the Ischia-Phlegrean geothermal fields, near Naples, from gravity and aeromagnetic data. Geophys. J., 97, 409-419.

Ridsdill-Smith, T.A. (2000). The Application of the Wavelet Transform to the Processing of Aeromagnetic Data (PhD thesis), University of Western Australia, pp. 197.

Rittman, A. (1930). Geologie der Insel Ischia. Zeitschrift fur Vulkanologie, Erganzungsband VI, Berlin, p. 268 (in German).

Roest, W.R., J. Verhoef and M. Pilkington (1992). Magnetic interpretation using the 3-D analytic signal. Geophysics, 57, 116-125.

Tibaldi, A. and L. Vezzoli (1998). The space problem of caldera resurgence: an example from Ischia Island, Italy. Geol. Rund, 87, 53-66.

Vezzoli, L. (1988). Island of Ischia. Quaderni de La Ricerca Scientifica, 114 (10), CNR, Progetto Finalizzato Geodinamica 10, Roma, 133 pp.

von Frese, R.R.B., M.B. Jones, J.W. Kim and W.S. Li (1997a). Analysis of anomaly correlations. Geophysics, 62(1), 342-351.

von Frese, R.R.B., M. B. Jones, J.W. Kim and W.S. Li (1997b). Spectral correlation of magnetic and gravity anomalies of Ohio. Geophysics, 62(1), 365-380.

*Corresponding author: Valeria Paoletti,
Department of Earth, Environment and Resources Science,
University Federico II, Naples, Italy;
email: paoletti@unina.it.